GNPy model of the physical layer for open and disaggregated optical networking [Invited]

JOURNAL OF
Optical Communications
and Networking

GNPy model of the physical layer for open and disaggregated optical networking [Invited]

VITTORIO CURRI

DET - Politecnico di Torino, Corso Duca degli Abruzzi, 24, Torino, Italy (curri@polito.it)

Received 4 January 2022; revised 20 March 2022; accepted 7 April 2022; published 4 May 2022

Networking technologies are fast evolving to support the request for ubiquitous Internet access that is becoming a fundamental need for the modern and inclusive society, with a dramatic speed-up caused by the COVID-19 emergency. Such evolution needs the development of networks into disaggregated and programmable systems according to the software-defined networking (SDN) paradigm. Wavelength-division multiplexed (WDM) optical transmission and networking is expanding as physical layer technology from core and metro networks to 5G *x*-hauling and inter- and intra-data-center connections requiring the application of the SDN paradigm at the optical layer based on the WDM optical data transport virtualization. We present the fundamental principles of the open-source project Gaussian Noise in Python (GNPy) for the optical transport virtualization in modeling the WDM optical transmission for open and disaggregated networking. GNPy approximates transparent lightpaths as additive white and Gaussian noise channels and can be used as a vendor-agnostic digital twin for open network planning and management. The quality-of-transmission degradation of each network element is independently modeled to allow disaggregated network management. We describe the GNPy models for fiber propagation, optical amplifiers, and reconfigurable add/drop multiplexers together with modeling of coherent transceivers from the back-to-back characterization. We address the use of GNPy as a vendor-agnostic design and planning tool and as physical layer virtualization in software-defined optical networking.

https://doi.org/10.1364/JOCN.452868

1. INTRODUCTION

As dramatically shown by the still ongoing pandemic emergency, access to the Internet is becoming a fundamental need for a modern and inclusive society [1,2]. Most of the working, educational, and recreational human life already partially relies on cloud applications and data storage, with a fast evolution toward the need for Internet access for most human activities [3,4].

Networking technologies are fast evolving to support the evolution toward the needed pervasive network architectures based on advanced wireless technologies seamlessly integrated with the optical transport. Specifically, with the 5G networking deployment evolving toward the 6G era, ultra-high-capacity radio access networks (RANs) exploiting multiple input multiple output and beam-forming technologies will be characterized by a very large amount of traffic per antenna. It requires optical fiber transmission and optical networking technologies to cover all network segments until the RAN front-haul [5], besides the already covered core- and metro-network segments. Moreover, inter-data-center wavelength-division multiplexed (WDM) optical connections are fast expanding to support cloud computing, requiring proper network management harmonized with the other network segments.

Such an evolution needs the full virtualization of network functions and hardware control to enable virtual slicing and programmable and dynamic adaptation of virtualized network operations to traffic and service requests [6]. For instance, 5G networking needs to rely on network slices granting ultra-low-latency connections.

The virtualization paradigm requires the disaggregation of telecommunications infrastructures into programmable multi-vendor network elements (NEs) and subsystems operated by open application program interfaces (APIs) and protocols within a hierarchical multi-layer network controller.

The industrial consortium Telecom Infra Project (TIP) is one of the consortia and standardization agencies operating with the purpose to develop open networking solutions. The TIP consortium groups most of the network operators and vendors to develop open software and hardware solutions for open networking. The TIP Open Optical and Packet Transport (OOPT) working group (WG) targets multi-layer solutions for open optical networking (OON) according to the partially disaggregated network architecture.

Optical networking is based on WDM optical circuits deployed and routed on the transparent optical infrastructure, so the OON needs a full virtualization of the physical layer to enable the optimal, dynamic, and software-defined exploitation of optical networks [7]. This is the purpose of the TIP project Gaussian Noise in Python (GNPy) that targets the development of an open-source software model of the WDM transport layer to be used as a digital twin of the optical infrastructure for design and planning and network management operations. The OOPT project GNPy is an open source software project [8] based on approximating as additive white Gaussian noise (AWGN) channels the transparent optical circuits—lightpaths (LPs)—operated by state-of-the-art dual-polarization coherent optical technologies. So, the physical layer is fully abstracted by the LP quality of transmission (QoT) summarized by the generalized signal-to-noise ratio (GSNR) including the effects of amplified spontaneous emission (ASE) noise from amplifiers and nonlinear interference (NLI) from fiber propagation [9]. The GNPy core is the QoT estimator that operates on the network topological graph and computes the GSNR on the selected wavelength on the given route—the selected LP—by accumulating the QoT impairments of each crossed NE.

In this paper, we summarize the concepts presented in [10] that are the fundamental bases of the GNPy project, and we then address its exploitation for open optical networking. The presented concepts are currently progressively implemented in the open-source repository of GNPy, so they do not refer to a specific software version. In general, we present theoretical assessments and models, and we do not address specific software implementations. It is worth remarking that a firm target of the GNPy project is to keep the computational time within a very limited number of computational cycles as requested by its use as a service within the network controller.

In Section 2, we review the disaggregated network architectures by focusing on the partially disaggregated architecture that is primarily targeted by the OOPT activities. In Section 3, we describe transmission models included in GNPy for each optical network element; then, in Section 4 we summarize as models are managed to utilize GNPy as a digital twin of the optical network. In Section 5, we comment on the use of GNPy as a vendor-neutral design and planning tool, while in Section 6, the use of GNPy for optical control and for lightpath computation in optical circuit deployment is described. Finally, Section 7 draws the general comments and conclusion.

2. DISAGGREGATED OPTICAL NETWORKS

The expansion of networking toward ubiquitous access to the Internet requires the evolution of networks from closed and *ossified* systems to open and programmable ecosystems, according to the software-defined networking (SDN) paradigm [11]. The evolution toward programmable networks needs the *disaggregation* of network architectures into independent and possibly multi-vendor network elements. Each disaggregated NE is a programmable white box exposing open models for its control and granting the virtualized access to its functionalities. NEs are controlled by a centralized multi-layer hierarchical network controller.

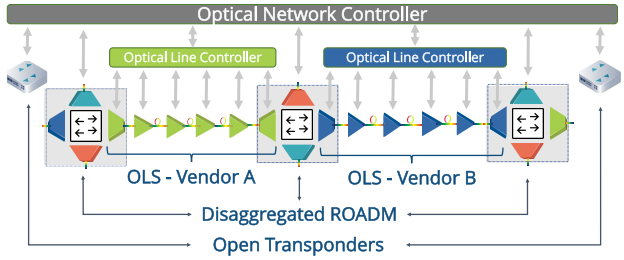

Fig. 1. Schematic block diagram for a partially disaggregated multi-vendor optical network architecture.

Optical communications and networking is expanding together with the 5G and future 6G deployment to support ultra-high-capacity wireless cells. Thus, WDM optical transport is expanding up to the RAN front-hauling, besides being the physical layer technology for core and metro networks, and inter- and intra-data-center connections. Consequently, along with wireless networking, optical networking is also required to evolve toward disaggregated and programmable architectures [12]. The main optical network elements are fibers, optical amplifiers (OAs), reconfigurable optical add/drop multiplexers (ROADM)s performing the optical switching operations, and transponders for deployment of optical circuits. Disaggregated optical networks can be classified as (a) fully disaggregated optical networks where each NE is independently controlled or (b) partially disaggregated optical networks where the amplified lines are managed as aggregated subsystems. The GNPy project targets the physical layer virtualization in partially disaggregated optical networks. As shown in Fig. 1, the optical network controller (ONC) manages the optical layer within a multi-layer hierarchical controller. The amplified lines connecting ROADMs may be independent WDM optical line systems (OLSs) [13–15], possibly multi-vendor, as pictorially described in Fig. 1. These ROADMs are operated in a disaggregated manner [16,17], where each degree, including the wavelength selective switches (WSSs), is disaggregated, implying that different directions may be independent OLSs from different vendors. Within a multi-layer hierarchical controller, each OLS is managed by an independent optical line controller (OLC) that sets the amplifiers' operational point.

The ONC has overarching control over the entire network. It computes and defines the paths of the optical tributary signals, sets the switching matrices in ROADMs, and manages all control and safety operations [13,14,17]. Traffic is loaded to the optical network by open transponders hosting pluggable transceivers (TRXs) that are fully controlled by the ONC by open interfaces [14,15,18].

3. OPTICAL TRANSPORT MODEL

In multi-layer networking, the optical data transport is a set of transparent WDM optical circuits to be optimally deployed and exploited. With an open and disaggregated approach to network planning and management, the optical transport must be virtualized as a network function to be used within the hierarchical controller.

The analysis of fiber propagation of a WDM channel comb is a complex problem due to nonlinear effects and stochastic

polarization-related phenomena. Thus, in general, the channel model for a transparent lightpath has to be accurately developed considering the transmission technique together with the physics of optical propagation. The use of dual-polarization (DP) coherent transceivers deploying multilevel modulation formats has dramatically simplified the scenario. Thanks to the compensation for linear propagation effects, including chromatic dispersion (CD), performed by the digital signal processing (DSP) in DP coherent TRXs, optical lines do not need dispersion compensating units and *ad hoc* optimized dispersion maps as were needed by intensity modulation with direct detection TRXs. This permits a full split-up of design and control of the optical infrastructure from the WDM optical data transport planning and management.

A major simplification in managing transmission is enabled by the dual-polarization nature of signals generated by coherent TRXs. Observing fiber propagation, we note that DP signals modulated at high symbol rates can be considered as depolarized signals over very short distances. This allows us to average out the stochastic nature of fiber polarization effects [19]. Prosecuting with the list of simplifications in propagation modeling enabled by DP coherent TRXs, we consider the fiber propagation phenomena. Coherent receivers compensate very well for all linear propagation effects (polarization rotations and chromatic dispersion), and thus the main residual QoT impairment of fiber propagation is the Kerr effect induced nonlinear cross talk: the NLI. Together with fiber propagation, the other QoT impairing network elements are the amplifiers adding the ASE noise and ROADMs introducing filtering penalty and polarization dependent loss (PDL). The accumulated statistics of polarization mode dispersion (PMD) and PDL must also be considered to include additional penalties.

It has been extensively demonstrated that the overall impact on channel performance of coherent optical signal propagation over transparent lightpaths can be reliably approximated by the insertion of an overall Gaussian noise disturbing the decision variable in the DSP [9]. This equivalent Gaussian disturbance includes both the ASE noise and NLI accumulated over the entire lightpath.

Therefore, when exploiting coherent optical technologies, physical effects in WDM optical data transport can be simplified by approximating transparent lightpaths as dual-polarization additive white and Gaussian noise channels as shown in Fig. 2. Thanks to this approximation, the QoT of a transparent lightpath can be summarized by its SNR, which is typically named generalized SNR [9,20,21] and is defined as

$$\mathrm{GSNR} = \frac{P_{\mathrm{CUT}}}{P_{\mathrm{ASE}} + P_{\mathrm{NLI}}} \cdot \mathrm{FP} = \frac{1}{\frac{1}{\mathrm{OSNR}} + \frac{P_{\mathrm{NLI}}}{P_{\mathrm{CUT}}}} \cdot \mathrm{FP}, \qquad (1)$$

where P_{CUT} is the power of the channel under test, and P_{ASE} and P_{NLI} are the accumulated ASE noise and NLI in the bandwidth B_n. FP is a factor ≤ 1 that accounts for the accumulated filtering penalty. $\mathrm{OSNR} = \mathrm{P_{CUT}}/\mathrm{P_{ASE}}$ is the optical SNR (OSNR). Note that the proper noise bandwidth for the GSNR definition is the symbol rate R_s of the channel under test, i.e., $B_n = R_s$, because the GSNR refers to the signal constellation after the application of the channel equalizer, including the matched filter.

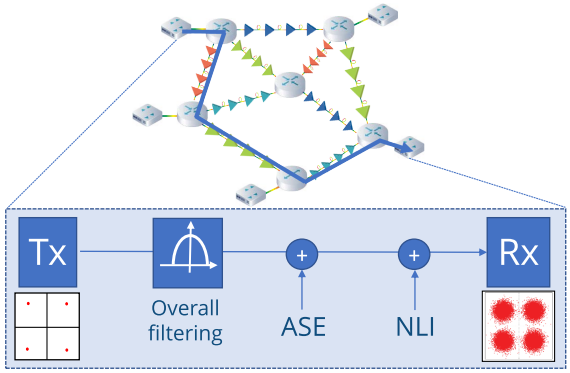

Fig. 2. Equivalent propagation impairments for propagation of dual-polarization coherent optical technologies over a transparent lightpath.

The AWGN channel approximation of transparent lightpaths enables the abstraction of optical circuits by a unique QoT parameter, the GSNR, while the performance of the coherent TRX can be summarized by a minimum requested GSNR. Consequently, the WDM physical layer abstraction can be easily managed provided that a proper modeling for the GSNR degradation of each optical NE is available. The QoT degradation model for each NE must provide the amount of gain/loss the element introduces on each WDM channel together with the possible amount of added noise, ASE or NLI. The LP GSNR is computed by accumulating the GSNR degradation introduced by each crossed NE [22] and can be compared to the TRX request to perform network planning and automatize control operations. Note that the AWGN channel approximation does not apply to the transmission of intensity modulated channels with direct detection.

In the following, we describe the main models for network elements, starting from TRXs.

A. Dual-Polarization Coherent Transceivers

Transceivers for DP coherent technologies *load* digital data on the optical carrier exploiting I/Q modulators driven by DSP-shaped signals. Coherent TRXs can be flexible, therefore enabling us to set operational modes based on different multilevel constellations with increasing cardinality and number of bits per symbol (BpS). The mostly exploited constellations are DP-QPSK (BpS = 4), DP-8QAM (BpS = 6), and DP-16QAM (BpS = 8). Larger cardinality constellations are also used for short-reach applications. Moreover, TRXs based on shaped constellations or hybrid formats are commercially available, allowing a fine-tuning of BpS. Given the symbol rate R_s, the corresponding net bit rate for data payload is $R_b = R_s \cdot \mathrm{BpS}/(1 + \mathrm{OH}/100)$, where OH is the code and protocol overhead expressed as a percentage of the net rate. Flexible TRXs may also allow different symbol rates and forward error correction (FEC) coding. Signals are typically shaped according to the raised-cosine power spectral density fully defined by the roll-off parameter α, and hence the actual signal spectral occupation is $B_s = R_s \cdot (1 + \alpha)$.

Assuming the AWGN channel model for transparent lightpaths, coherent TRXs can be fully characterized in back-to-back (b2b) setups by mimicking the channel impact by

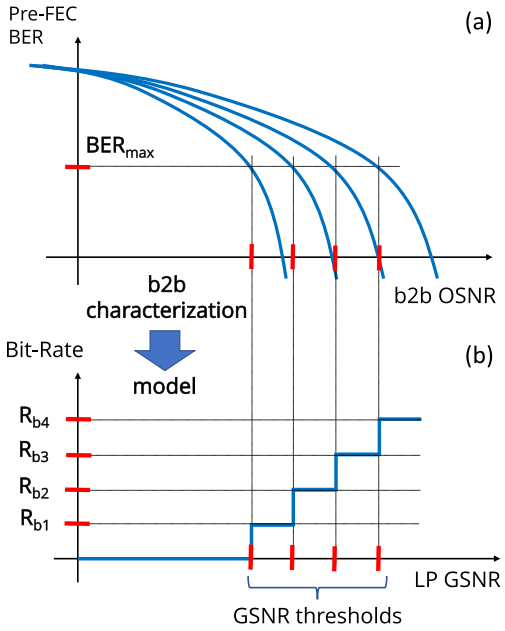

Fig. 3. Qualitative plot for the b2b characterization of a flexible TRX (a) to obtain the lightpath GSNR thresholds (b) for the available modulation formats.

ASE noise loading. As an example, in Fig. 3, a qualitative plot for a four modulation format (MF) flexible TRX is depicted. For each available MF, in a b2b setup, the pre-FEC bit error rate (BER) can be collected versus the OSNR by loading ASE noise. Thus, a set of curves with a monotone decreasing behavior as qualitatively shown in Fig. 3(a) is obtained. Given the exploited FEC technology, a BER threshold BER_{max} is defined, and consequently a set of OSNR thresholds requested for each available MF for *in-service* operation is derived. Considering the AWGN channel as a model for propagation over transparent lightpaths, the OSNR thresholds obtained from the b2b characterization can be considered as GSNR thresholds. These are the GSNRs requested for the transparent LP to reliably deploy each of the available MFs and the corresponding bit rate. Following this approach to model flexible TRXs, the information needed from the network controller to compute the lightpath feasibility are the following: from the TRX model, the spectral occupation B_s, the GSNR thresholds, and the corresponding bit rates; from the network digital twin, the available wavelength continuity and bandwidth; and for QoT, the computation of the available GSNR.

Because of the electrical noise in the TRX, the b2b characterization to obtain the GSNR thresholds must be available at different received power levels within the TRX operational range. So, a complete TRX model for GSNR thresholds includes the variation of each threshold with the received power level. Therefore, the TRX threshold data structure $GSNR_{th}$ is a $N_{OM} \times N_{PRX}$ matrix, where N_{OM} is the number of TRX operational modes and N_{PRX} is the number of received power levels used in the characterization. Such power levels are included in the $GSNR_{th}$ data structure as well.

The main QoT impairment is given by the noise added in propagation, but other impacts must also be considered for a complete TRX model. Besides noise, the most important

Operational Mode	Modulation Format	Symbol Rate [Gbaud]	Roll off	Bit Rate [Gbps]	GSNR Thresholds [dB]	Max CD [ps/nm]
Mode 1	MF_1	R_{s1}	α_1	R_{b1}	$GSNR_{th,1}$	CD_{max1}
...	...	...	...		....	...
Mode N	MF_N	R_{sN}	α_N	R_{bN}	$GSNR_{th,N}$	CD_{maxN}

Fig. 4. Simplified TRX model for virtualized management of optical transceivers.

propagation effect to be considered is the CD. CD is typically very well compensated for by the DSP, but it needs very large memory that implies larger cost and larger power consumption for TRXs. Lower-cost and lower-power-consumption solutions for TRX are commercially available for short-reach applications with limited CD compensation capability. Thus, the maximum amount of chromatic dispersion that the TRX can compensate for must be part of the TRX model. A more detailed TRX model may include a table for GSNR penalty versus accumulated CD. The other possible impairments to be considered in modeling TRXs are caused by the accumulated PMD [23] from fiber spans and PDL [24] from ROADMs and OAs. Both are statistical effects varying with time, and the impact on performance depends on DSP algorithms, so a proper GSNR penalty model needs a stochastic approach based on the statistics of the accumulated effect and the maximum tolerable outage probability [25] as commented below in Section 3.C.

To summarize, a comprehensive model for dual-polarization coherent TRXs must include for each supported modulation format the BER versus OSNR b2b characterization and the GSNR penalty curves for the accumulated CD, PMD, and PDL. To simplify lightpath deployment, a model based on thresholds can be used as shown in Fig. 4. From the information exposed in this table, the network controller can fully manage the TRX within the network digital twin by comparing the channel spectral occupation, the requested GSNR, and the maximum tolerable CD to the available bandwidth, the GSNR, and the introduced CD on the selected lightpath. The model presented in Fig. 4 can be further improved by considering a progressive GSNR penalty with CD ($GSNR_{pen,CD}$) instead of a single maximum tolerable value, and by addressing PMD and PDL penalties ($GSNR_{pen,PMD}$ and $GSNR_{pen,PDL}$). By including these penalties, the *effective* GSNR threshold will be $GSNR_{th,eff} = GSNR_{th} + GSNR_{pen,CD} + GSNR_{pen,PMD} + GSNR_{pen,PDL}$ [dB].

B. Optical Amplifiers

Optical fibers are transmission media introducing very low power loss in propagation. In modern fibers, it is given by the fundamental scattering laws [26] and is lower than 0.2 dB/km in the C band. Despite such excellent performance, the loss introduced by fibers and connectors must be periodically recovered by OAs. The standard technology used for amplification in the C and L bands is the erbium-doped fiber amplifier (EDFA). Technologies exploiting other rare-earth elements are under development to obtain amplification beyond the C + L band.

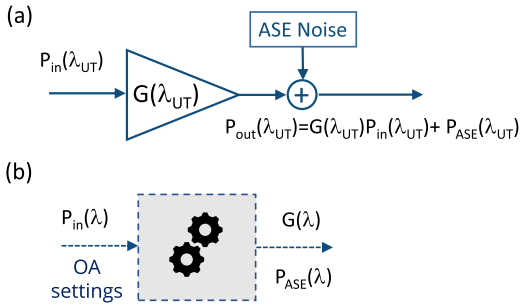

Fig. 5. Model for virtualized management of optical dual-polarization coherent transceivers.

Modeling physical phenomena in EDFAs is complex and requires full knowledge of the internal device structure [27], but such a level of detail is not required for transmission and networking analyses. As shown in Fig. 5(a), the propagation effect of amplifiers is conceptually simple: it is well modeled by the introduction of some ASE noise degrading the OSNR together with the gain. Thus, to compute the QoT impairment of amplifiers on a channel under test at the wavelength λ_{UT}, the only needed EDFA models are for the gain $G(\lambda_{UT})$ and the amount of ASE noise $P_{ASE}(\lambda_{UT})$ added in the signal bandwidth. The ideal OA model is displayed in Fig. 5(b), i.e., a model that, given the input power spectral density $P_{in}(\lambda)$ and the OA settings (typically, gain or power operational mode, target gain/power and tilt), provides the gain $G(\lambda)$ and amount of added ASE noise $P_{ASE}(\lambda)$. Such an accurate model is typically not available; practically, the OA model is provided as an approximation at full spectral load (all WDM channels on at the OA input) of the gain curve $G(\lambda)$ together with the noise figure $F(\lambda)$. The amount of noise is consequently computed as [27]

$$P_{ASE}(\lambda) = F(\lambda)[G(\lambda) - 1]hfR_s, \quad \textbf{(2)}$$

where h is the Plank's constant and $f = c/\lambda$.

In all practical scenarios, it is always convenient to control the amplifiers in order to keep the amount of ASE noise dominant with respect to the NLI introduced by fiber propagation [28]. Moreover, power levels at the input of fiber spans exciting the Kerr effect are given by the amplifier gain, including its variation with wavelength. Therefore, a model for OAs with precise spectral resolution is a fundamental need for an accurate and reliable abstraction of the optical physical layer. To this purpose, machine learning models can be effectively exploited [29] also to include the effects of partial spectral load at the OA input. These models can be provided by vendors together with the hardware as trained machine-learning agents [29] or can be trained in the field by the network operator on the installed amplified line exploiting ASE-shaped generators and channel monitors as proposed in [30].

C. Fiber Propagation

The effect of fiber propagation on WDM dual-polarization coherent channel combs has been extensively analyzed in the past years. Considering that coherent receivers fully compensate for fiber propagation linear effects and apply the matched filter, several mathematical models of physical effects have been proposed and validated. All derivations apply a perturbative approach and aim at describing the nature of the residual impairments after the equalized coherent receiver [31,32] that is typically called nonlinear interference. These mathematical models can be classified in two main categories.

- *Aggregated* models.

These target the *exact* evaluation of the NLI generated by the entire optically amplified line, so they include spatial transients and modulation format dependence. These models need full knowledge and control of the transmission line, including for each fiber span, full awareness of side channels (modulation format and amount of accumulated CD) propagating together with the channel under test. These models can be used in the optimization of point-to-point transmission, while they are not suitable for disaggregated network management. The original models were proposed in [33,34].

- *Disaggregated* models.

These aim at the evaluation of the worst-case amount of NLI independently induced by each fiber span and are modulation-format agnostic. The original disaggregated model is the well-known GN model described in [35]. These mathematical models can be used for the abstraction of the optical layer with a disaggregated approach, as they need only local knowledge and do not require detailed information on each propagating channel.

Independently of the specific approach, all theoretical derivations show that the effect of WDM fiber propagation can be summarized by the introduction of the NLI disturbance caused by the nonlinear Kerr effect interacting with the chromatic dispersion and the attenuation. Such a disturbance, considered after the full chromatic dispersion compensation applied by the adaptive receiver, together with the matched filter and the carrier phase recovery, at the optimal sampling time, has been extensively demonstrated to be well characterized as a dual-polarization additive Gaussian random process [36].

The wave equation for fiber evolution of the modal amplitude is the coupled nonlinear Shrödinger equation [37], which is a stochastic equation, as it includes the random birefringence. Focusing on the analysis of propagation of DP coherent optical technologies, the propagating optical signal is depolarized over short propagation distances, so we can apply a polarization average to the wave equation. Moreover, the PMD is generally compensated for by adaptive coherent receivers and weakly interacts with NLI generation [38]. Hence, we can use as the fiber wave equation the Manakov equation [19] centered at the wavelength of the channel under test.

The WDM spectrum is the comb of DP spectrally orthogonal N_{ch} statistically independent random processes. Substituting such a signal form in the Manakov equation, we obtain a set of N_{ch} wave equations, each including loss, chromatic dispersion, and self- and cross-channel nonlinear effects: the spectrally separated Manakov equation (SSME). Nonlinear effects are always a perturbation in WDM optical transmission, so each channel is assumed to propagate according to the following perturbative law:

$$\bar{A}_i(f, z) = \left\{\bar{A}_i(f, 0) + \bar{N}_i(f, z)\right\}\sqrt{p_i(z)}H_{D,i}(f, z), \quad \textbf{(3)}$$

where f is the frequency and z is the propagation distance. $\bar{A}_i(f,z)=[A_{x,i},A_{y,i}]^T$ is the optical field amplitude of the ith channel under test, $p_i(z)$ is the power evolution including loss and stimulated Raman Scattering (SRS) [39] effects, $H_{D,i}(f,z)$ is the effect of chromatic dispersion, and $\bar{N}_i(f,z)=[N_{x,i},N_{y,i}]^T$ is the NLI spectrally centered on the ith channel. Substituting Eq. (3) into the SSME, a set of differential equations is obtained for the generation of the N_{ch} $\bar{N}_i(f,z)$ components. Integrating the equations and relying on the statistical properties of digital signals, the power spectral density $G_{N,i}(f)$ of $\bar{N}_i(f,z)$ can be evaluated. The coherent receiver autonomously applies the matched filter, so the NLI Gaussian random process intensity impairing the decision signal is $P_{\text{NLI},i}=\int_{-\infty}^{+\infty}G_{N,i}(f)|H_m(f)|^2\mathrm{d}f$. Different mathematical models proposed in the literature rely on different approaches and approximations for the $P_{\text{NLI},i}$ computation, but all can be summarized in the following common form:

$$P_{\text{NLI},i}=\eta_{\text{SPM},i}P_i^3+P_i\sum_{j\neq i}\eta_{\text{XPM},ij}P_j^2+\sum_{klm\in\text{FWM}_i}\eta_{\text{FWM},iklm}P_kP_lP_m, \tag{4}$$

where P_i is the input power of the ith channel; FWM_i is the set of four wave mixing (FWM) indices klm on the ith channel; and $\eta_{\text{SPM},i}$, $\eta_{\text{XPM},i}$, and $\eta_{\text{FWM},iklm}$ are the efficiency for self-phase modulation, cross-phase modulation, and FWM, respectively, generating the self-, cross-, and multi-channel NLI components. For most practical scenarios, FWM is negligible, so the NLI components can be spectrally separated. Aggregated mathematical models focus on ηs computation integrating the differential equation for $N_i(f,z)$ on the entire link and for a given propagating channel comb, while the disaggregated NLI models aim at the evaluation of the equivalent NLI generated by each fiber span and by each WDM channel on the channel under test.

In order to obtain an accurate QoT evaluation, as for the OA model, also for the NLI generation, variations with f must be considered, starting with the loss coefficient. This becomes a firm request in the case of multi-band transmission beyond the C band. An effective method to properly consider variations with f of loss is to rely on the phenomenological expansion proposed in [26]

$$\alpha(\lambda)\simeq\alpha_{\text{S}}(\lambda)+\alpha_{\text{UV}}(\lambda)+\alpha_{\text{IR}}(\lambda)+\alpha_{13}(\lambda), \tag{5}$$

where $\alpha_{\text{S}}(\lambda)$, $\alpha_{\text{UV}}(\lambda)$, $\alpha_{\text{IR}}(\lambda)$, and $\alpha_{13}(\lambda)$ are the Rayleigh scattering, ultraviolet, infrared, and OH^- peak absorption contributions, respectively.

The other propagation effect that must be accurately considered for an accurate QoT is the SRS [39]. The SRS impairment on WDM signal combs is a seamless transferring of optical power from higher to lower frequencies depending on the frequency spacing Δf, with the efficiency peak at Δf around 12 THz [39]. The effect of SRS on per-channel power evolution must be accurately evaluated given the power spectral density at the fiber input by solving the SRS set of N_{ch} differential equations [40]:

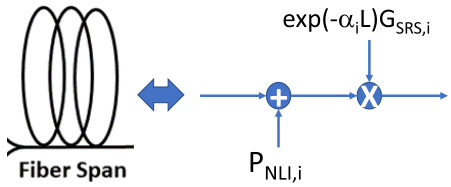

Fig. 6. Equivalent fiber effect on the ith channel of each fiber span as considered within GNPy.

$$\frac{\partial P_n(z)}{\partial z}=-\alpha_nP_n(z)-P_n(z)\sum_{m=1}^{n-1}C_R(f_n;\Delta f_{\text{nm}})P_m(z)+P_n(z)\sum_{m=n+1}^{N_{\text{ch}}}C_R(f_m;\Delta f_{\text{mn}})P_m(z), \tag{6}$$

where $P(z)$ is the power evolution of the nth channel centered at f_n in the N_{ch} WDM channel comb, α_n is the loss coefficient for the nth channel, $\Delta f_{\text{nm}}=f_n-f_m$, and $C_R(f_n;\Delta f_{\text{nm}})$ is the Raman efficiency referred to f_n for the spectral separation Δf_{nm}. To get an accurate evaluation of SRS, a proper shape for the Raman profile and its scaling with the reference frequency must be considered [39]. Given the input power per channel $P_n=P_n(0)$, the solution of Eq. (6) is the per-channel power evolution $P_n(z)=P_n\cdot p_n(z)=P_n\exp(-\alpha_nz)G_{\text{SRS},n}(z)$. To include the frequency variations in the NLI evaluation, the GN model has been generalized by considering the SRS and loss profile [21,41,42].

To model the NLI generation in GNPy, a disaggregated implementation of the generalized GN model is considered and modified to include the correlation [43] in the accumulation of the self-channel NLI component. So, the per-channel NLI generated by each fiber span is expressed as

$$P_{\text{NLI},i}=(1+C_\infty)\eta_{\text{SPM},i}P_i^3+P_i\sum_{j\neq i}\eta_{\text{XPM},ij}P_j^2, \tag{7}$$

where C_∞ is the SC-NLI correlation coefficient and $\eta_{\text{SPM},i}$ and $\eta_{\text{XPM},ij}$ are evaluated considering the exact per channel power evolution $\exp(-\alpha_nz)G_{\text{SRS},n}(z)$ with $n=i$ and $n=j$, respectively [44]. For each channel, the propagation on each fiber span is considered as pictorially described in Fig. 6. This approach to the NLI modeling is well known to be conservative yet accurate for long-haul transmission that is typically limited by the joint effect of ASE noise and NLI. In few- and single-span links, the model may considerably overestimate the NLI, but in such transmission scenarios the NLI is typically negligible, even if overestimated, with respect to other transmission impairments, starting from the TRX electrical noise. So, the overall accuracy in performance predictions is typically also very good in these scenarios. In any case, the model architecture may in perspective include more accurate NLI modeling if needed by specific applications.

Besides considering the NLI, other additive metrics must be computed and accumulated in propagation on each fiber span to be used by the TRX model. These are the accumulated chromatic dispersion $D_{\text{acc},i}=D_i\cdot L_{\text{span}}$ [ps/nm], the squared PMD $\Delta\tau^2=\delta_{\text{PMD}}^2\cdot L_{\text{span}}$ [ps^2], and the latency $\Delta T=n/c\cdot L_{\text{span}}\simeq 5\cdot L_{\text{span}}$ [μsec]. L_{span} [km] is the fiber

span length, D_i [ps/nm/km] is the chromatic dispersion coefficient for the ith WDM channel, δ_{PMD} [ps/$\sqrt{\text{km}}$] is the fiber PMD coefficient, $n \simeq 1.5$ is the fiber refractive index, and c is the speed of light. Note that the PMD is a time-varying stochastic effect whose related probability density function for the introduced differential group delay (DGD) accumulated over a lightpath is a Maxwellian distribution [23]. The PMD cumulative metric is the DGD variance, so the related maximum tolerable PMD in the TRX model (see Section 3.A) is set by a maximum tolerable outage probability [25]. Another stochastic effect is the accumulated PDL whose impact can be severe in metro network segments including several ROADMs. The PDL impact was analyzed for intensity modulated channels [45], while the impairment on DP coherent optical technologies needs further investigations to define the cumulative metric and the statistics of the induced TRX penalties, following a stochastic approach as for the PMD.

A final comment is needed on modeling optical fiber spans including Raman pumping to obtain Raman amplification. To properly consider this scenario, a more complete version of Eq. (6) must be used [40] by including bidirectional SRS interactions for co- and counter-propagating pumps. From this mathematical modeling, we obtain the G_{SRS} including both the inter-channel SRS and gain together with the added ASE noise generated by the spontaneous emission. In the presence of Raman pumping, the fiber model depicted in Eq. (6) is updated by also adding the SRS ASE noise. Moreover, $G_{\text{SRS},i}$ also includes the effect of Raman gain. It is worth noting that in most practical scenarios it is inconvenient to exploit co-propagating pumps and in general to rely on full-Raman amplification [46]. Practically, counter-propagating Raman pumping is extensively used to assist EDFAs and to reduce the noise figure of the overall hybrid amplifier. In these scenarios, the excess NLI generated by the distributed amplification is typically negligible, so Raman amplification can be modeled as an equivalent lumped OA as described in Section 3.B. $G(\lambda)$ is the *on-off* Raman gain, and the ASE noise $P_{\text{ASE}}(\lambda)$ is defined by the spontaneous emission computation from the fiber SRS equations.

D. Reconfigurable Optical Add/Drop Multiplexers

In transparent optical infrastructures, network elements implementing the fundamental networking operation are ROADMs. ROADMs are in charge of adding/dropping optical circuits and of transparently routing the optical circuits carrying *express* traffic. Regardless of the specific exploited technologies, ROADMs can be described as schematically shown in Fig. 7(a), following a disaggregated approach. ROADMs are classified according to the number of degrees. Each degree is connected to a bidirectional fiber pair that is the ingress/egress of an amplified optical line. Each degree includes WSS structures, one for the degree ingress and another for the degree egress. WSSs are $1 \times N_W$ devices able to switch any input wavelength or portion of the spectrum to any of the N_W outputs, if used in the 1-to-N_W direction, or to combine the wavelengths on the N_W inputs in the single output, if used in the opposite direction. As described in Section 2, according to the partially disaggregated networking paradigm, each ROADM degree

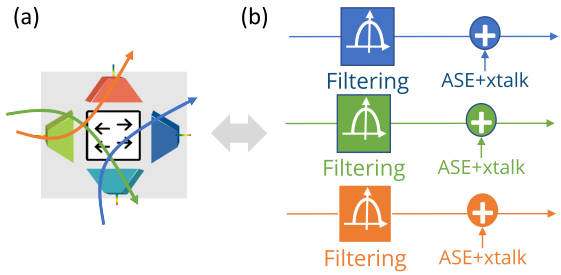

Fig. 7. (a) Disaggregated ROADM architecture and (b) transmission model for different routed wavelengths.

is the ingress/egress of an independent WDM optical line system. ROADMs include one add/drop degree connected to the optical TRXs that are terminals for transparent optical circuits. N_d degrees are assembled to build a N_d-degree ROADM implementing a N_dxN_dxN_{WDM} transparent optical switching matrix, where N_{WDM} is the number of WDM wavelengths used in transmission.

Ideal ROADMs are colorless directionless contentionless (CDC) structures; i.e., they are able to route any wavelength from any fiber input to any fiber output regardless of the direction of the wavelength and of the switching matrix. The complexity of CDC ROADM structures grows dramatically with the number of degrees N_d, so practically ROADMs are designed according to simplified structures including some contention effect. ROADMs may include a couple of EDFAs on each degree that with a disaggregated and open approach can be considered as a booster or pre-amplifier of the amplified optical line and can be modeled independently as described in Section 3.B.

From a transmission model viewpoint, the ROADM effect on QoT of transparently routed or added/dropped wavelengths is conceptually simple. As pictorially depicted in Fig. 7(b), given a switching path that must be allowed by the ROADM structure in the case of a non-CDC ROADM, the main impairment is the filtering effect. Moreover, some disturbances can be added. These are some ASE noise from possible amplification devices (e.g., semiconductor optical amplifiers) in the switches and cross talk from side channels and residual dropped channels. Cross talk can be assumed as a Gaussian disturbance that adds up to the ASE noise and depends on the spectral shape of the channel. The filtering effect is a linear degradation that accumulates over transparent lightpath propagation including the contribution $H_i(f)$ of each of the N crossed filtering network elements. The overall LP filtering transfer function $\prod_{i=1}^{N} H_i(f)$ is compensated for by the channel equalizer. The effect is a GSNR degradation that in general depends on the modulation format and on the specific DSP implementation of a coherent receiver. As a consequence, in general, the filtering effect model is the full transfer function $H_i(f)$ relating the filtering elements to be considered together with the filtering effect on the overall accumulated ASE noise. In the case of limited filtering effect, as expected in practical scenarios, it has been experimentally shown [47] that the GSNR degradation can be characterized independently on each filtering element as $F_{P,i}$ [dB], and the resulting lightpath GSNR penalty is $F_P \simeq \sum_{i=1}^{N} F_{P,i}$

[dB]. Filtering penalties so evaluated have to be considered as expected values of random processes because of uncertainties in filters inducing randomness.

For a complete ROADM model, another required piece of information is the power levels requested at the ROADM input and provided at the ROADM output. These power levels must be specified as power spectral densities, i.e., power in a reference bandwidth, to enable flex-grid flex-rate network management [48]. In summary, a complete ROADM model gets as inputs the switching path and the TRX model and provides the GSNR degradation and filtering penalty together with the I/O power spectral densities. The complexity of the model varies dramatically with the complexity of the ROADM structure and with the ROADM technologies. With the evolution toward the use of photonics integrated circuits and the need for more complex switching structures, machine learning can be a useful solution for ROADM models [49]. Another possibly relevant impairment of ROADMs is the introduced PDL that must be accumulated statistically as commented in Sections 3.A and 3.C.

4. OPTICAL NETWORK DIGITAL TWIN

The optical transport model implemented in GNPy has been extensively tested in experimental results. In [20], GNPy was tested in a green field scenario using a large set of multi-vendor TRXs, and in [21] the validation was extended to a full C-band mixed-fiber scenario including Raman amplification. In [50], GNPy has been tested for the first time in a brown field scenario, while in [48] the results of a test in a multi-vendor flex-rate flex-grid scenario are presented, including the TRX using shaped constellations. In [51], GNPy has been validated for a Nyquist subcarrier TRX [52] with a bit rate up to 800 Gbits/s. Therefore, the GNPy modeling has been extensively validated to be reliably used as a digital twin of the optical WDM layer in open optical networking. To this purpose, the fundamental need is for accurate models of network elements. Therefore, each NE is required to be exposed by open interface propagation models as described in Section 3. Exact parameters describing fiber cables are also a fundamental request. These can be provided by the network operator or can be retrieved autonomously from network monitors as proposed in [53].

In Fig. 8, we pictorially describe the concept of a digital twin of an optical network given by GNPy. It is the network topological graph where graph nodes are ROADMs and graph

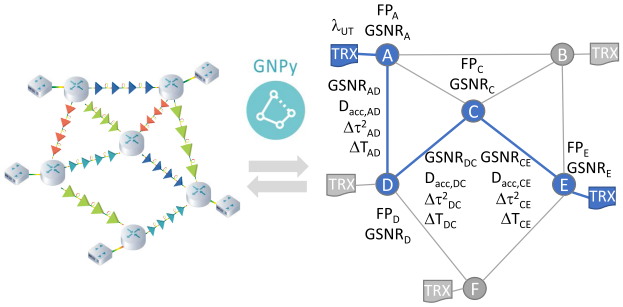

Fig. 8. Digital twin of an optical network by GNPy. A sample lightpath for λ_{UT} is highlighted together with the computed metrics on crossed ROADMs and OLSs.

edges are OLSs. On the graph, we can identify any route, as, for instance, "ADCE" highlighted in Fig. 8, and compute the TRX performance at λ_{UT} over the specified route. Given the TRX and NE models, and the spectral loads on every OLS, GNPy evaluates the metrics of the crossed OLSs and ROADMs and computes the accumulated metrics for the lightpath under test [22]. For the GSNR, the additive metric is the inverse GSNR in linear units, so the LP GSNR in dB units is

$$\mathrm{GSNR}_{\mathrm{LP}} = 10\log_{10}\left[\left(\sum_{\mathrm{LP}}\frac{1}{\mathrm{GSNR}_i}\right)^{-1}\right]\ [\mathrm{dB}]\,, \tag{8}$$

where GSNR_i is the GSNR degradation in linear units induced by every ith crossed element over the lightpath. The OLS GSNR degradation is the sum of contributions induced by each OA and fiber span in the OLS. The GSNR is computed for a channel at λ_{UT} according to the TRX model. It is worth remarking that, besides models of network elements, for path computation, the spectral load on every OLS must be specified together with the control strategy of the OAs. The other LP metric related to the QoT is the filtering penalty. If the FP induced by each element is limited [47], the additive FP metric is the per-element FP_i in dB units, so the LP FP is

$$\mathrm{FP}_{\mathrm{LP}} = \sum_{\mathrm{LP}}\mathrm{FP}_i[\mathrm{dB}], \tag{9}$$

where FP_i is the filtering penalty provided by the model of each ith crossed ROADM at λ_{UT} for the channel described in the TRX model. Given the LP GSNR and FP, the effective GSNR to be compared to the GSNR thresholds from the TRX model is

$$\mathrm{GSNR}_{\mathrm{eff}} = \mathrm{GSNR}_{\mathrm{LP}} - \mathrm{FP}_{\mathrm{LP}}[\mathrm{dB}]. \tag{10}$$

For the accumulated CD, the additive metric is the CD introduced by each fiber span $D_{\mathrm{acc},i} = D_i L_{\mathrm{span},i}$, so the accumulated CD over the LP is

$$D_{\mathrm{LP}} = \sum_{\mathrm{LP}} D_{\mathrm{acc},i}\left[\frac{\mathrm{ps}}{\mathrm{nm}}\right]. \tag{11}$$

For the PMD statistics, the cumulative metric is

$$\Delta\tau_{\mathrm{LP}} = \sqrt{\sum_{\mathrm{LP}}\Delta\tau_i^2}[\mathrm{ps}], \tag{12}$$

where $\Delta\tau_i^2 = \delta^2_{\mathrm{PMD}}$ and $L_{\mathrm{span},i}$ are the contributions of each crossed fiber span. Finally, each LP is also characterized by a crucial metric for ultra-low-latency networking that is the propagation latency defined as

$$\Delta T_{\mathrm{LP}} = \sum_{\mathrm{LP}}\Delta T_i[\mathrm{ms}], \tag{13}$$

where ΔT_i are the propagation delays introduced by the crossed fiber spans.

The optical network digital twin can be used for network design and planning as the engine of a vendor-neutral planning tool. It can also be used within the hierarchical network

controller as a service to enable software-defined optical networking, specifically, to support optical control and to assist optical circuit computation and deployment. It is worth remarking that the optical layer full virtualization enables virtual slicing and possible sharing of optical infrastructures.

5. GNPy ASSISTED NETWORK DESIGN AND PLANNING

The fundamental request for the progress of open and disaggregation networking deployment from demo to production scenarios is for vendor-neutral design and planning tools. These tools will enable multi-vendor solutions to be virtually tested and compared in the network design phase.

GNPy can be used as a vendor-neutral design tool for optical networks to virtually compare performance of different optical layer design solutions [54]. To this purpose, vendors must provide GNPy models for network elements as described in Section 3, so operators can use the metrics provided by GNPy simulations as shown in Section 4 to benchmark and challenge bidders' designs. GNPy metrics can be integrated by techno-economics analyses for a cost-effective network design process. A practical example has been the use of GNPy in the West African backbone project [55].

Besides supporting the entire network design, GNPy can be exploited to virtually test possible networking upgrades. For instance, operators may virtually test the feasibility of new TRX solutions (e.g., 400ZR) on the deployed network infrastructure before proceeding with experimental testing. This approach may evolve toward software-defined optical network architectures based on an independent optical transport infrastructure that exposes its digital twin for optical circuit deployment [18].

Besides its use as design and planning tool in commercial contexts, GNPy can be exploited in R&D for networking simulations including full awareness of the physical layer. The impact on the networking performance of different approaches can be compared to steer the development of novel transmission solutions. Examples are the use of GNPy to investigate multi-band networking [56] or to generate synthetic yet realistic datasets for machine-learning assisted networking [57].

6. GNPy IN SOFTWARE DEFINED OPTICAL NETWORKING

Software-defined networking [11] is a network architecture where control of network elements is directly programmable and decoupled from traffic management. According to the SDN paradigm, network elements are fully virtualized within the network controller as *southbound* common application program interfaces. According to the SDN approach, network functions implemented by *programmable* network elements are virtualized as *northbound* APIs. The SDN implementation needs a *common language* for interfaces from hardware and control software, so it needs common open protocols and data models. Therefore, the progressive implementation of the SDN paradigm is steered by standardization agencies and consortia.

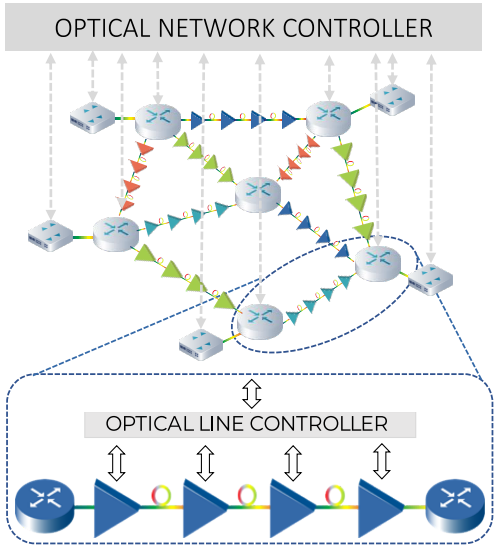

Fig. 9. Software-defined optical control in a partially disaggregated optical network.

The SDN architecture was first proposed for the packet network layer [11]; then, it extended toward the physical layer, including optical networking [7]. In the SDN multi-layer hierarchical controller, we can identify the ONC in charge of managing the optical networking: hardware control and optical circuit management. According to the SDN paradigm, these operations must be decoupled.

In Fig. 9, we schematically depict the software-defined optical network application for a partially disaggregated optical network. Every ROADM-to-ROADM OLS is controlled by an independent OLC that sets the operational point of OAs. The OLC has a local ROADM-to-ROADM vision and is traffic agnostic. The related OLS may be either open or closed. In the case of an open OLS, the OLC controls devices and exposes the line model as a *white box* to the ONC. The OLC has full access to each device and implements the control algorithm specified by the ONC to set the operational point of OAs. On the contrary, in closed OLSs, the OLC exposes to the ONC the line as a *black box* providing only the metrics required for the line abstraction within the digital twin: GSNR degradation, accumulated CD, PMD, PDL, and propagation latency. The control algorithm implemented in the OLC is not exposed.

The optical network controller has a *global* vision of the transparent network infrastructure and, besides interacting with the OLC, needs full control of the network elements in charge of optical circuit management. These are transceivers and ROADMs that must be open white boxes enabling full control of the device functionalities. The ONC, when a source-to-destination optical circuit is requested, finds the proper route and wavelength, performs the optical path computation on the LP QoT, sets the switching matrices, and deploys the optical circuit by setting the TRX operational mode. Within the OOPT activities of the Telecom Infra Project, working groups including operators and vendors work to develop the open ecosystem for multi-layer software-defined optical networking. In the following, we describe the use of

GNPy as a service for optical control and for optical circuit management.

A. Optical Control

The optical control algorithm implemented by the OLC targets the operational point of the line OAs to minimize the QoT degradation, on each wavelength in the optical transmission band, given the constraints of the available OAs. The OA setting procedure implies transients and possible *out-of-service* events, so the OLC status is typically reset rarely, mostly in the case of hardware failures, as for recovery from fiber cuts. The OLC algorithm must be traffic agnostic and targets the optimization in the worst-case traffic scenario, i.e., the OLS operating at full WDM spectral load.

According to the approximation of transparent lightpaths as AWGN channels, the contribution of each OLS on the LP QoT is defined by its GSNR degradation. Consequently, the optimal algorithm can be mathematically formalized as the optimization of the GSNR computed on the OLS supposed to be operated at full WDM spectral load. Considering a simplified model for OAs supposing spectrally flat gain together with a spectrally flat and gain-independent noise figure, the problem has a simple solution as shown in [28,58]. In general, the frequency dependence of the GSNR must be considered. It is caused by fiber propagation (loss profile and SRS effect) and by OAs whose models are generally more complex than the spectrally flat model. In general, the OLS GSNR varies with the frequency and depends on the OA settings—the optimization space for the control algorithm—and on the line input power spectral density (PSD) defined by the ingress ROADM and the line output PSD required by the egress ROADM. Hence, the OLC target is to maximize the average GSNR in the transmission band together with the minimization of the GSNR variations. We need to minimize the GSNR(f) variations with the frequency in order to guarantee for the entire set of WDM channels in the transmission band similar QoT in propagation over the OLS. This allows larger flexibility in LP deployment across several OLSs, avoiding bottlenecks due to the absence of wavelength continuity on a few high-performing wavelengths. Thus, the problem of line optimization in the space of *OA settings* of each OA can be formalized as

$$\begin{cases} \max\limits_{\text{OA settings}} & \left\{\overline{\text{GSNR}_{\text{OLS}}}\right\} \\ \min\limits_{\text{OA settings}} & \left\{\left\langle\left(\text{GSNR}_{\text{OLS}}(f)-\overline{\text{GSNR}_{\text{OLS}}}\right)^2\right\rangle\right\} \\ P_{\text{OLS,in}}(f) & = P_{\text{ROADM,out}}(f) \\ P_{\text{OLS,out}}(f) & = P_{\text{ROADM,in}}(f) \end{cases}, \quad \textbf{(14)}$$

where $\overline{\text{GSNR}} = \langle \text{GSNR}(f) \rangle$ and $\langle \cdots \rangle$ is the average in the transmission band.

As shown in Fig. 10, GNPy can serve as a digital twin of the OLS only. It provides to the line optimizer algorithm the GSNR(f) at full WDM spectral load with different OA settings to be used for the optimization of Eq. (14). Regardless of the specific optimization algorithm, the fundamental need to obtain accurate and reliable results is the accurate line description including fibers, connectors, and spectrally resolved OA models. For the OAs, it is crucial to have an accurate model

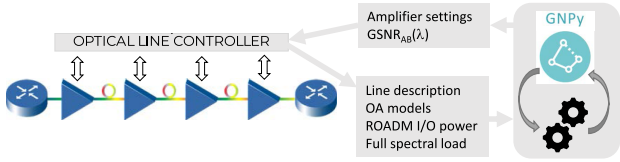

Fig. 10. Architecture for the optical line controller using GNPy.

including the characterization of the available working modes and settings. In [53], an experimental proof of concept is shown where the OLC autonomously identifies fibers and connectors from optical channel monitors and sets the amplifier operational point by using GNPy within a genetic algorithm optimizer.

B. Optical Circuit Deployment

A transparent optical network is a circuit-switched network where circuits are transparent lightpaths from a defined source s to a defined destination d carrying digital data connections at the bit rate jointly defined by the TRX and by the LP QoT. Given the network topology, the physical layer description, the transmission band, and the WDM grid, we can define as *route space* the set of all potentially available lightpaths. With the progressive network loading, the available lightpaths in the *route space* decrease because of the progressive spectral occupation.

Thanks to the digital twin, the operation of optical circuit deployment can be fully automatized. The optical network controller has a global vision of the network topology, controls TRXs and ROADMs, and gets line models from the optical line controller. Moreover, the ONC is aware of the deployed circuits and in general of the network status. Therefore, the ONC can provide to the GNPy all the needed data to virtualize the network.

In LP deployment, in flex-grid WDM, the first operation is the routing wavelength and spectral assignment (RWSA) that identifies the available wavelength and bandwidth over a topological route for circuit deployment. Thanks to GNPy, given an s-to-d connection request, the RWSA operation can be fully virtualized within the digital twin with full knowledge of the LP metrics. With a full virtualization of the optical network, the route space can be virtually sliced, so the RSWA operation may operate on different subsets of the route space, according to the service constraints (e.g., low-latency traffic). Once the RSWA has identified the LP, as shown in Fig. 11, GNPy performs optical path computation by providing the LP metrics as described in Section 4. Thanks to the control on TRX settings and to the models of the TRX in s and d nodes, the ONC sets the TRX operational mode and consequently the circuit bit rate by comparing the LP GSNR$_{\text{eff}}$ from the optical path computation to the effective GSNR$_{\text{th}}$ from the TRX models. With respect to the definition of Eq. (10), GSNR$_{\text{eff}}$ can be further reduced by the system margin μ. The other LP metrics (e.g., the accumulated chromatic dispersion, PMD, and PDL) can also be considered for TRX settings. Recently, experimental proofs of concept on the use of GNPy in optical circuit deployment have been presented in [59–61].

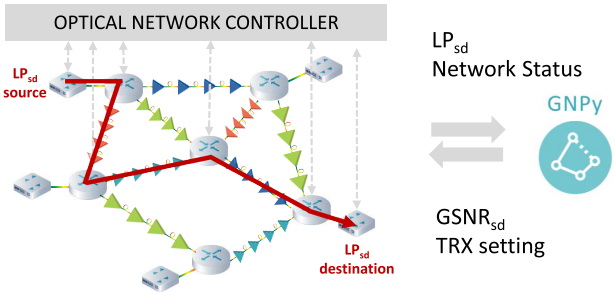

Fig. 11. Architecture for the optical path computation and TRX setting using GNPy.

In LP deployment, the effective GSNR to be used for TRX setting must be the worst-case value to avoid *out-of-service* events due to GSNR degradation in progressive traffic deployment. Thus, the GSNR degradation by each OLS must be evaluated at full spectral load to maximize the interference among channels in fiber propagation. Special attention must be addressed to the EDFAs, whose behavior is strongly dependent on the spectral load, in cases of a limited number of active channels with respect to the full spectral load. Therefore, by relying on the digital twin, the ONC can also virtually test the actual LP $\mathrm{GSNR}_{\mathrm{eff}}$ for the specific network loading. It enables us to verify that the EDFA behavior with low channel load does not reduce the $\mathrm{GSNR}_{\mathrm{eff}}$ below the nominal value computed at full spectral load. This operation needs accurate and spectral-load-dependent OA models. To this purpose, machine learning models may be effectively exploited by GNPy as shown by the experimental proof of concept presented in [30]. The final yet fundamental comment on the optical path computation is about the role of uncertainties in physical layer description. The main sources of uncertainties in cables are connector and splice losses in fibers. These are in general not well characterized by network monitors and may vary in time because of human operations and recovery from fiber cuts. Other sources of uncertainties are ripples in the gain and noise figure of amplifiers and filtering penalties. Consequently, the estimated $\mathrm{GSNR}_{\mathrm{eff}}$ in optical path computation must be considered together with a confidence interval $\pm\Delta_{\mathrm{GSNR}}$. Without a statistical characterization of variations of $\mathrm{GSNR}_{\mathrm{eff}}$, the needed minimum system margin is $\mu = \Delta_{\mathrm{GSNR}}$. An accurate statistical regression from physical layer uncertainties on the variations of the actual effective GSNR with respect to the predicted value $\mathrm{GSNR}_{\mathrm{eff}}$ would enable the statistical definition of system margin μ based on the maximum tolerable out-of-service probability P_{OOS}: $P\{\mathrm{GSNR} \le \mathrm{GSNR}_{\mathrm{eff}} - \mu\} \le P_{\mathrm{OOS}}$.

7. CONCLUSION

We have presented the modeling approach to the WDM optical transport abstraction implemented in the open-source project GNPy by the consortium Telecom Infra Project. We described the partially disaggregated optical network architecture that is the application framework for GNPy. We showed that in such a context, transparent lightpaths can be approximated as AWGN channels affected by the ASE noise from amplifiers and NLI from fiber propagation, together with filtering penalties. Additional penalties may be caused by the accumulated CD, PMD, and PDL. Such a modeling approach allows us to virtualize the optical network within GNPy as a network digital twin where the QoT impairments are accumulated by adding up the degradation introduced by each network element. We commented on how GNPy can be used as a vendor-agnostic design and planning tool to virtually test different multi-vendor solutions. Then, we described the exploitation of GNPy as a service within the SDN multi-layer hierarchical controller to implement the optical line control and to assist the open and automatic deployment of optical circuits.

Funding. H2020 Marie Skłodowska-Curie Actions (814276).

Acknowledgment. The author thanks the Telecom Infra Project OOPT-PSE working group and the PLANET research team at Politecnico di Torino. This project has been supported by the Telecom Infra Project and by the European Union's Horizon 2020 Marie Skłodowska-Curie ETN-ITN Wideband Optical Networks.

REFERENCES

1. P. Soto-Acosta, "COVID-19 pandemic: shifting digital transformation to a high-speed gear," Inf. Syst. Manag. **37**, 260–266 (2020).
2. T. Böttger, G. Ibrahim, and B. Vallis, "How the Internet reacted to Covid-19: a perspective from Facebook's edge network," in *ACM Internet Measurement Conference* (Association for Computing Machinery, 2020).
3. F. Almeida, J. D. Santos, and J. A. Monteiro, "The challenges and opportunities in the digitalization of companies in a post-COVID-19 world," IEEE Eng. Manag. Rev. **48**, 97–103 (2020).
4. S. Keesara, A. Jonas, and K. Schulman, "Covid-19 and health care's digital revolution," New England J. Med. **382**, e82 (2020).
5. N. Al-Falahy and O. Y. Alani, "Technologies for 5G networks: challenges and opportunities," IT Prof. **19**, 12–20 (2017).
6. S. Abdelwahab, B. Hamdaoui, M. Guizani, and T. Znati, "Network function virtualization in 5G," IEEE Commun. Mag. **54**(4), 84–91 (2016).
7. A. S. Thyagaturu, A. Mercian, M. P. McGarry, M. Reisslein, and W. Kellerer, "Software defined optical networks (SDONs): a comprehensive survey," IEEE Commun. Surv. Tutorials **18**, 2738–2786 (2016).
8. "GitHub repository of GNPy," https://doi.org/10.5281/zenodo.3458319.
9. A. Pilipetskii, D. Kovsh, E. Mateo, E. R. Hartling, G. Mohs, L. Jovanovski, M. Salsi, M. Cantono, M. Bolshtyansky, O. Courtois, O. Gautheron, O. A. Sab, P. Pecci, P. Mehta, S. Grubb, T. Inoue, V. Kamalov, V. Vusirikala, V. Letellier, and Y. Inada, "The subsea fiber as a Shannon channel," in *Proceedings of SubOptic* (2019).
10. V. Curri, "GNPy model for design of open and disaggregated optical networks," in *European Conference on Optical Communication (ECOC)* (2021).
11. W. Xia, Y. Wen, C. H. Foh, D. Niyato, and H. Xie, "A survey on software-defined networking," IEEE Commun. Surv. Tutorials **17**, 27–51 (2015).
12. E. Le Rouzic, O. Augizeau, O. Renais, J. Meuric, T. Marcot, C. Betoule, G. Thouenon, A. Triki, M. Laye, N. Pelloquin, Y. Lagadec, and E. Delfour, "Automation journey in core and metro networks: an operator view," in *European Conference on Optical Communication (ECOC)* (2021).
13. S. Gringeri, B. Basch, V. Shukla, R. Egorov, and T. J. Xia, "Flexible architectures for optical transport nodes and networks," IEEE Commun. Mag. **48**(7), 40–50 (2010).
14. E. Riccardi, P. Gunning, Ó. G. de Dios, M. Quagliotti, V. López, and A. Lord, "An operator view on the introduction of white boxes into optical networks," J. Lightwave Technol. **36**, 3062–3072 (2018).
15. C. Manso, R. Muñoz, N. Yoshikane, R. Casellas, R. Vilalta, R. Martínez, T. Tsuritani, and I. Morita, "TAPI-enabled SDN control

for partially disaggregated multi-domain (OLS) and multi-layer (WDM over SDM) optical networks," J. Opt. Commun. Netw. **13**, A21–A33 (2021).
16. J. Kundrát, O. Havliš, J. Jedlinski, and J. Vojtěch, "Opening up ROADMs: let us build a disaggregated open optical line system," J. Lightwave Technol. **37**, 4041–4051 (2019).
17. M. Birk, O. Renais, G. Lambert, C. Betoule, G. Thouenon, A. Triki, D. Bhardwaj, S. Vachhani, N. Padi, and S. Tse, "The openROADM initiative," J. Opt. Commun. Netw. **12**, C58–C67 (2020).
18. H. Nishizawa, W. Ishida, Y. Sone, T. Tanaka, S. Kuwabara, T. Inui, T. Sasai, and M. Tomizawa, "Open whitebox architecture for smart integration of optical networking and data center technology," J. Opt. Commun. Netw. **13**, A78–A87 (2021).
19. D. Marcuse, C. Manyuk, and P. Wai, "Application of the Manakov-PMD equation to studies of signal propagation in optical fibers with randomly varying birefringence," J. Lightwave Technol. **15**, 1735–1746 (1997).
20. M. Filer, M. Cantono, A. Ferrari, G. Grammel, G. Galimberti, and V. Curri, "Multi-vendor experimental validation of an open source QoT estimator for optical networks," J. Lightwave Technol. **36**, 3073–3082 (2018).
21. A. Ferrari, M. Filer, K. Balasubramanian, Y. Yin, E. Le Rouzic, J. Kundrát, G. Grammel, G. Galimberti, and V. Curri, "GNPy: an open source application for physical layer aware open optical networks," J. Opt. Commun. Netw. **12**, C31–C40 (2020).
22. V. Curri, "Software-defined WDM optical transport in disaggregated open optical networks," in *22nd International Conference on Transparent Optical Networks* (2020).
23. G. Foschini and C. Poole, "Statistical theory of polarization dispersion in single mode fibers," J. Lightwave Technol. **9**, 1439–1456 (1991).
24. A. El Amari, N. Gisin, B. Perny, H. Zbinden, and C. Zimmer, "Statistical prediction and experimental verification of concatenations of fiber optic components with polarization dependent loss," J. Lightwave Technol. **16**, 332–339 (1998).
25. H. Bulow, "System outage probability due to first- and second-order PMD," IEEE Photon. Technol. Lett. **10**, 696–698 (1998).
26. S. Walker, "Rapid modeling and estimation of total spectral loss in optical fibers," J. Lightwave Technol. **4**, 1125–1131 (1986).
27. E. Desurvire, *Erbium-Doped Fiber Amplifiers: Principles and Applications* (Wiley, 2002).
28. V. Curri, A. Carena, A. Arduino, G. Bosco, P. Poggiolini, A. Nespola, and F. Forghieri, "Design strategies and merit of system parameters for uniform uncompensated links supporting Nyquist-WDM transmission," J. Lightwave Technol. **33**, 3921–3932 (2015).
29. J. Yu, S. Zhu, C. L. Gutterman, G. Zussman, and D. C. Kilper, "Machine-learning-based EDFA gain estimation," J. Opt. Commun. Netw. **13**, B83–B91 (2021).
30. A. D'Amico, S. Straullu, G. Borraccini, E. London, S. Bottacchi, S. Piciaccia, A. Tanzi, A. Nespola, G. Galimberti, S. Swail, and V. Curri, "Enhancing lightpath QoT computation with machine learning in partially disaggregated optical networks," IEEE Open J. Commun. Soc. **2**, 564–574 (2021).
31. A. Mecozzi and R.-J. Essiambre, "Nonlinear Shannon limit in pseudolinear coherent systems," J. Lightwave Technol. **30**, 2011–2024 (2012).
32. R. Dar, M. Feder, A. Mecozzi, and M. Shtaif, "Properties of nonlinear noise in long, dispersion-uncompensated fiber links," Opt. Express **21**, 25685–25699 (2013).
33. A. Carena, G. Bosco, V. Curri, Y. Jiang, P. Poggiolini, and F. Forghieri, "EGN model of non-linear fiber propagation," Opt. Express **22**, 16335–16362 (2014).
34. R. Dar, M. Feder, A. Mecozzi, and M. Shtaif, "Accumulation of nonlinear interference noise in fiber-optic systems," Opt. Express **22**, 14199–14211 (2014).
35. P. Poggiolini, G. Bosco, A. Carena, V. Curri, Y. Jiang, and F. Forghieri, "The GN-model of fiber non-linear propagation and its applications," J. Lightwave Technol. **32**, 694–721 (2014).
36. A. Bononi, O. Beucher, and P. Serena, "Single- and cross-channel nonlinear interference in the Gaussian noise model with rectangular spectra," Opt. Express **21**, 32254–32268 (2013).
37. G. Agrawal, *Nonlinear Fiber Optics*, 5th ed. (Academic, 2013).
38. M. Cantono, D. Pilori, A. Ferrari, A. Carena, and V. Curri, "Observing the interaction of PMD with generation of NLI in uncompensated amplified optical links," in *Optical Fiber Communication Conference (OFC)* (2018), paper W1G.4.
39. K. Rottwitt, J. Bromage, A. J. Stentz, L. Leng, M. E. Lines, and H. Smith, "Scaling of the Raman gain coefficient: applications to germanosilicate fibers," J. Lightwave Technol. **21**, 1652–1662 (2003).
40. J. Bromage, "Raman amplification for fiber communications systems," J. Lightwave Technol. **22**, 79–93 (2004).
41. M. Cantono, D. Pilori, A. Ferrari, C. Catanese, J. Thouras, J.-L. Augé, and V. Curri, "On the interplay of nonlinear interference generation with stimulated Raman scattering for QoT estimation," J. Lightwave Technol. **36**, 3131–3141 (2018).
42. D. Semrau, R. I. Killey, and P. Bayvel, "The Gaussian noise model in the presence of inter-channel stimulated Raman scattering," J. Lightwave Technol. **36**, 3046–3055 (2018).
43. A. D'Amico, E. London, E. Virgillito, A. Napoli, and V. Curri, "Quality of transmission estimation for planning of disaggregated optical networks," in *International Conference on Optical Network Design and Modeling (ONDM)* (2020).
44. A. D'Amico, B. Correia, E. London, E. Virgillito, G. Borraccini, and V. Curri, "Scalable and disaggregated GGN approximation applied to a C+L+S optical network," J. Lightwave Technol. (to be published).
45. A. Mecozzi and M. Shtaif, "Signal-to-noise-ratio degradation caused by polarization-dependent loss and the effect of dynamic gain equalization," J. Lightwave Technol. **22**, 1856–1871 (2004).
46. V. Curri and A. Carena, "Merit of Raman pumping in uniform and uncompensated links supporting NyWDM transmission," J. Lightwave Technol. **34**, 554–565 (2016).
47. T. Rahman, A. Napoli, D. Rafique, B. Spinnler, M. Kuschnerov, I. Lobato, B. Clouet, M. Bohn, C. Okonkwo, and H. de Waardt, "On the mitigation of optical filtering penalties originating from ROADM cascade," IEEE Photon. Technol. Lett. **26**, 154–157 (2014).
48. A. D'Amico, E. London, B. Le Guyader, F. Frank, E. Le Rouzic, E. Pincemin, N. Brochier, and V. Curri, "Experimental validation of GNPy in a multi-vendor flex-grid flex-rate WDM optical transport scenario," J. Opt. Commun. Netw. **14**, 79–88 (2022).
49. I. Khan, L. Tunesi, M. U. Masood, E. Ghillino, P. Bardella, A. Carena, and V. Curri, "Automatic management of $N \times N$ photonic switch powered by machine learning in software-defined optical transport," IEEE Open J. Commun. Soc. **2**, 1358–1365 (2021).
50. A. Ferrari, K. Balasubramanian, M. Filer, Y. Yin, E. Le Rouzic, J. Kundrát, G. Grammel, G. Galimberti, and V. Curri, "Softwarized optical transport QoT in production optical network: a brownfield validation," in *European Conference on Optical Communications (ECOC)* (2020).
51. A. D'Amico, B. Le Guyader, F. Frank, E. Le Rouzic, E. Pincemin, A. Napoli, H. Sun, B. Spinnler, N. Brochier, and V. Curri, "GNPy experimental validation for Nyquist subcarriers flexible transmission up to 800 G," in *Optical Fiber Communication Conference (OFC)* (2022), paper M4F.6.
52. D. Welch, A. Napoli, J. Bäck, W. Sande, J. Pedro, F. Masoud, C. Fludger, T. Duthel, H. Sun, S. J. Hand, T.-K. Chiang, A. Chase, A. Mathur, T. A. Eriksson, M. Plantare, M. Olson, S. Voll, and K.-T. Wu, "Point-to-multipoint optical networks using coherent digital subcarriers," J. Lightwave Technol. **39**, 5232–5247 (2021).
53. G. Borraccini, A. D'Amico, S. Straullu, A. Nespola, S. Piciaccia, A. Tanzi, G. Galimberti, S. Bottacchi, S. Swail, and V. Curri, "Cognitive and autonomous QoT-driven optical line controller," J. Opt. Commun. Netw. **13**, E23–E31 (2021).
54. J.-L. Auge, G. Grammel, E. Le Rouzic, V. Curri, G. Galimberti, and J. Powell, "Open optical network planning demonstration," in *Optical Fiber Communication Conference (OFC)* (2019), paper M3Z.9.
55. TIP, "Orange steps towards open optical networks with GNPy," 2020, https://telecominfraproject.com/orange-steps-towards-open-optical-networks-with-gnpy/.
56. B. Correia, R. Sadeghi, E. Virgillito, A. Napoli, N. Costa, J. Pedro, and V. Curri, "Networking performance of power optimized C+L+S multiband transmission," in *IEEE Global Communications Conference (GLOBECOM)* (IEEE, 2020).

57. Z. Zhong, M. Ghobadi, M. Balandat, S. Katti, A. Kazerouni, J. Leach, M. McKillop, and Y. Zhang, "BOW: first real-world demonstration of a Bayesian optimization system for wavelength reconfiguration," in *Optical Fiber Communication Conference (OFC)* (2021), paper F3B.1.
58. R. Pastorelli, S. Piciaccia, G. Galimberti, E. Self, M. Brunella, G. Calabretta, F. Forghieri, D. Siracusa, A. Zanardi, E. Salvadori, G. Bosco, A. Carena, V. Curri, and P. Poggiolini, "Optical control plane based on an analytical model of non-linear transmission effects in a self-optimized network," in *39th European Conference and Exhibition on Optical Communication (ECOC)* (IET, 2013).
59. G. Borraccini, S. Straullu, A. Ferrari, E. Virgillito, S. Bottacchi, S. Swail, S. Piciaccia, G. Galimberti, G. Grammel, and V. Curri, "Using QoT-E for open line controlling and modulation format deployment: an experimental proof of concept," in *European Conference on Optical Communications (ECOC)* (2020).
60. J. Kundrát, E. Le Rouzic, J. Mårtensson, A. Campanella, O. Havliš, A. D'Amico, G. Grammel, G. Galimberti, V. Curri, and J. Vojtěch, "GNPy & YANG: open APIs for end-to-end service provisioning in optical networks," in *Optical Fiber Communication Conference (OFC)* (2021), paper M1B.6.
61. TIP, "First demonstration of TIP Phoenix at NTT R&D Forum," https://telecominfraproject.com/first-demo-tip-phoenix-ntt-rd-forum/.